Supplementary Figure 1

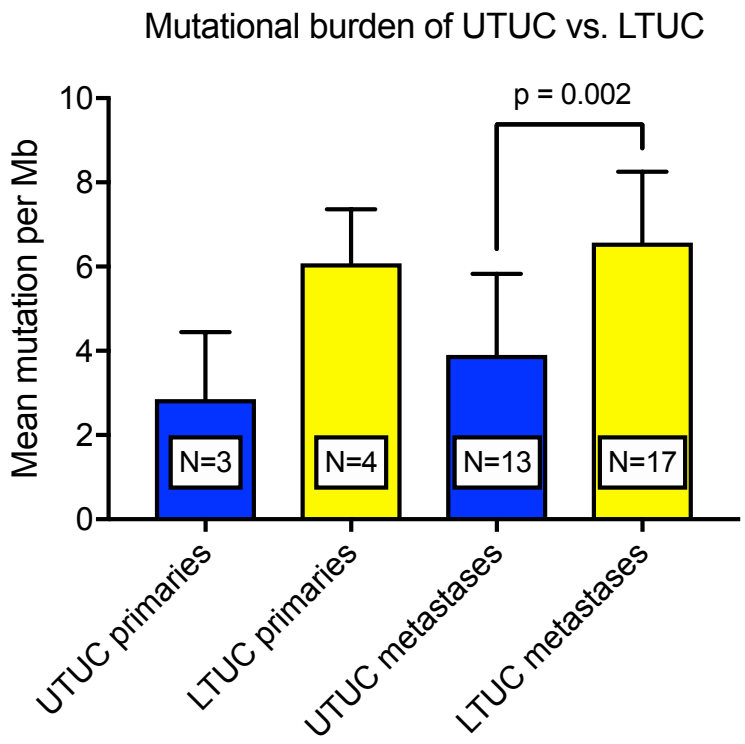

Supplementary Figure 1. Overall mutational burden of each sequenced tumor stratified by UTUC and LTUC, and primary vs. metastatic tumors.
Numbers analyzed for each as shown (p-value for metastatic samples calculated using Mann-Whitney-U test). No p-value provided for the primary specimens given the small sample size. However, the trend demonstrates a lower mutational frequency in UTUC compared to LTUC. Data presented as mean +/- SD.

Supplementary Figure 2

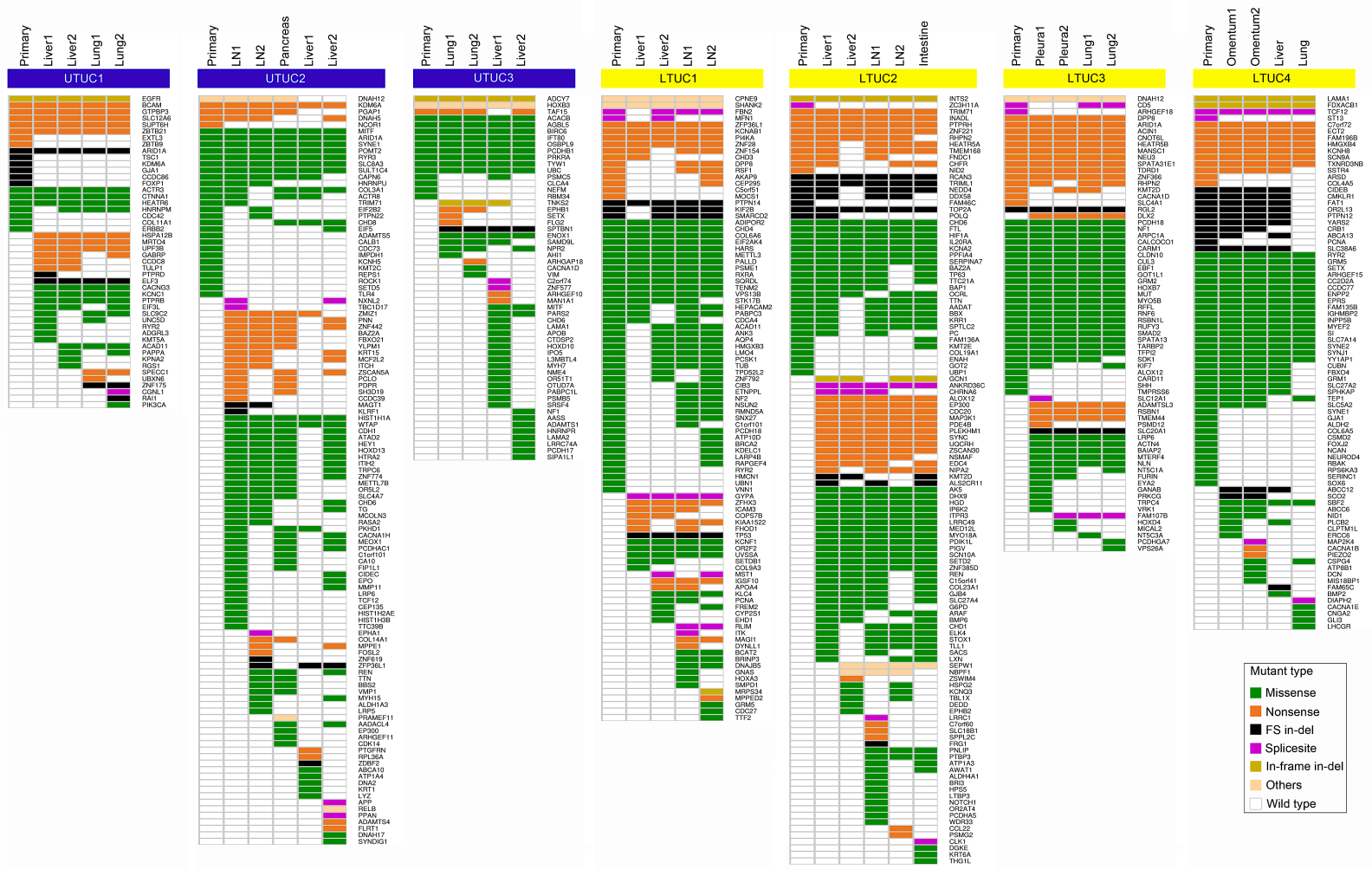

Supplementary Figure 2. Predicted deleterious mutation distribution across LTUC and UTUC primary and metastatic tumors.

Supplementary Figure 3

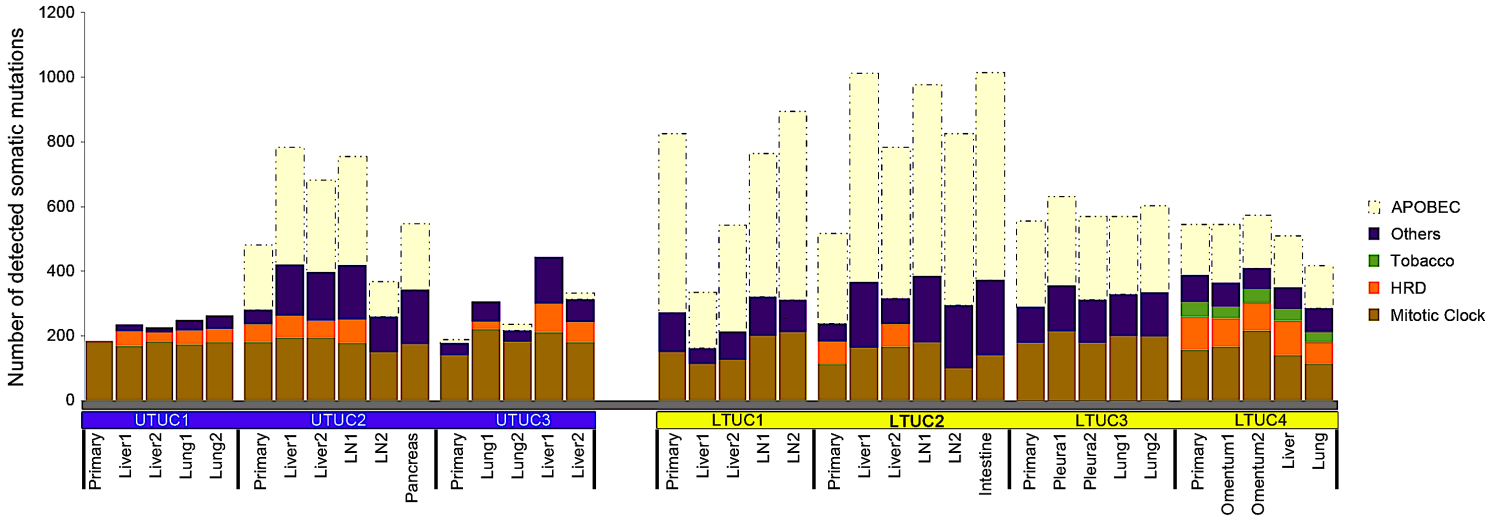

Supplementary Figure 3. Mutational signature analysis with predominant APOBEC signature removed reveals similar mutational burden across UTUC and LTUC samples.

Mutational signature analysis across each primary and metastatic UTUC and LTUC tumor specimen represented as an absolute number of all mutations within a given tumor. All mutation analyses were performed following baseline read filtering (see methods). HRD: Homologous recombination deficiency; APOBEC: Apolipoprotein B mRNA, Catalytic Polypeptide; Mitotic clock: age-related signature changes.

Supplementary Figure 4

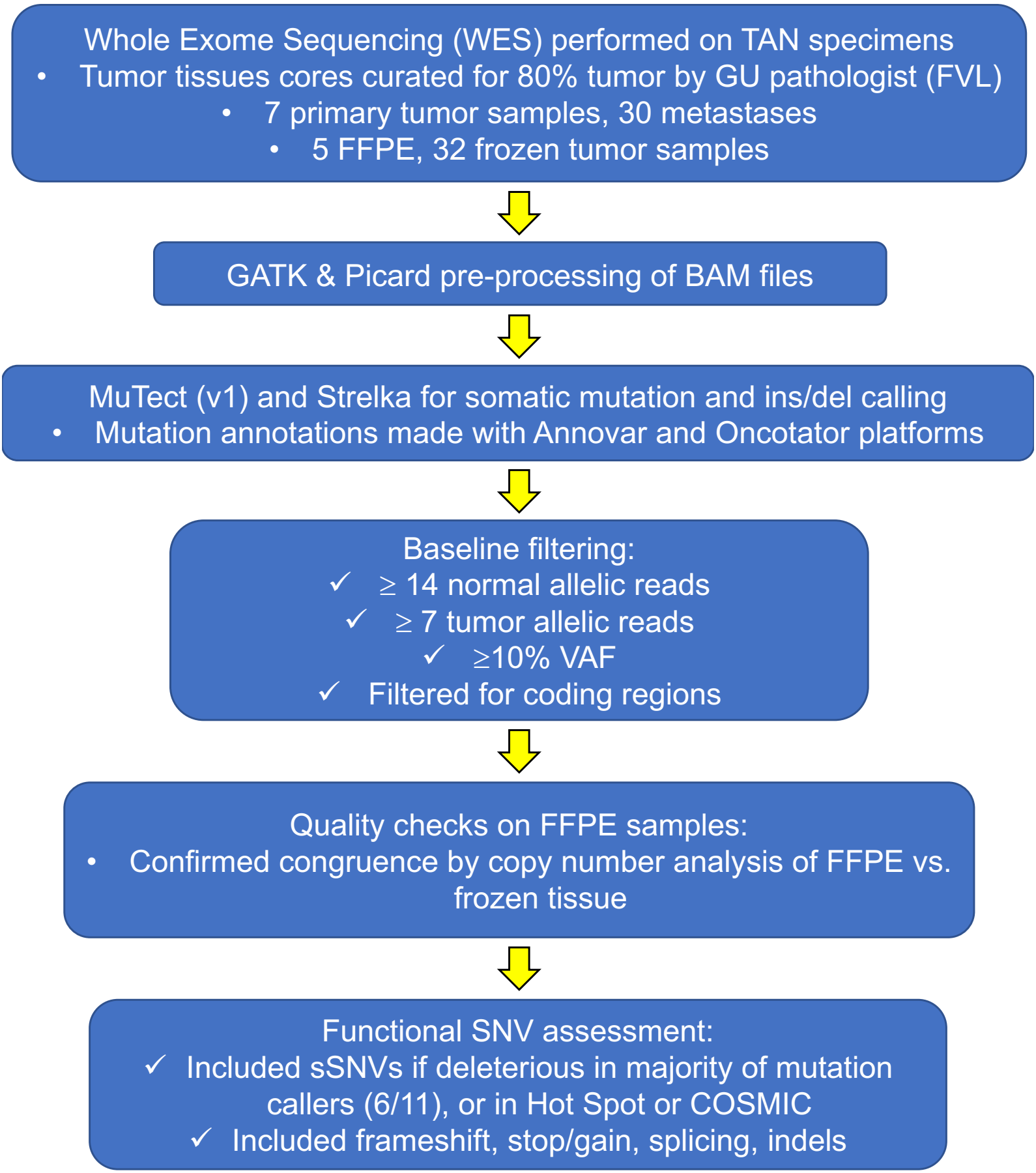

Supplementary Figure 4. Schematic for predicted deleterious mutation calling.

Supplementary Figure 5

Supplementary Figure 5. Power analysis of all sSNV identified across each specimen within each patient.

Supplementary Figure 6

Primary tumor

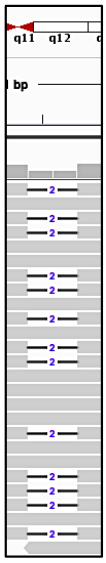

Frameshift mutation:
Chr1:27107094

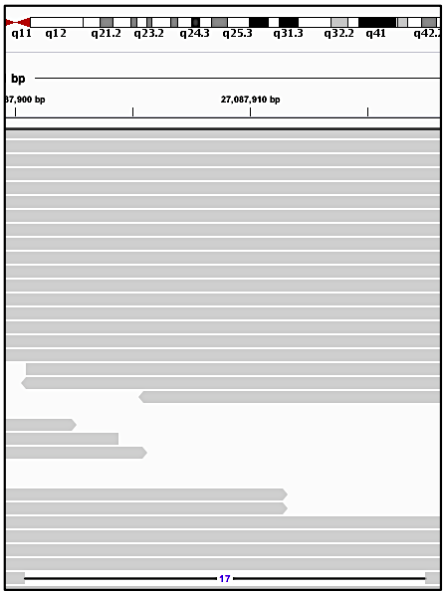

Frameshift mutation 2:
Chr1:27087900

Metastatic tumors

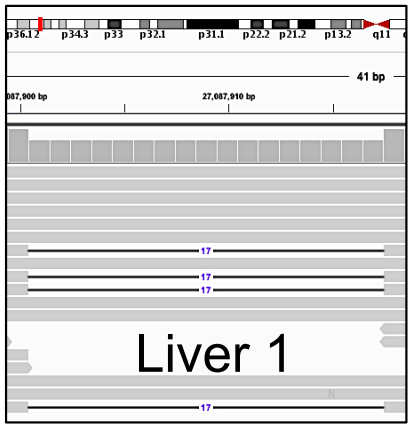

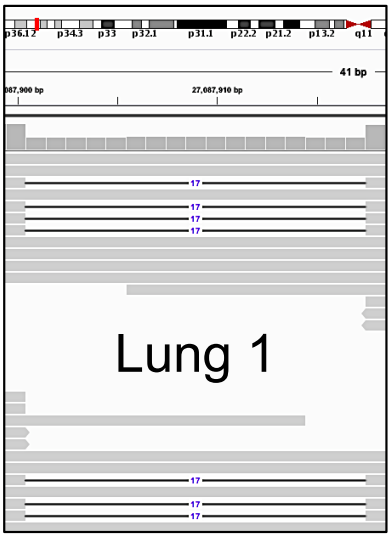

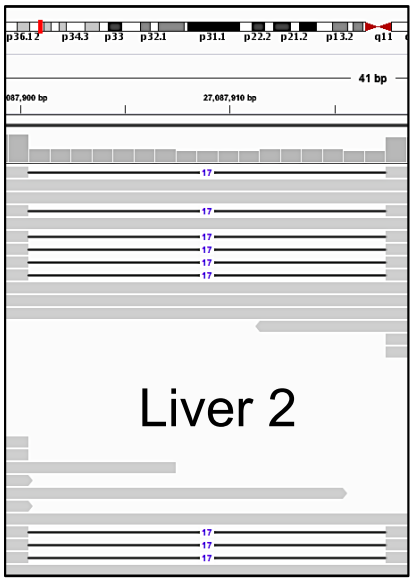

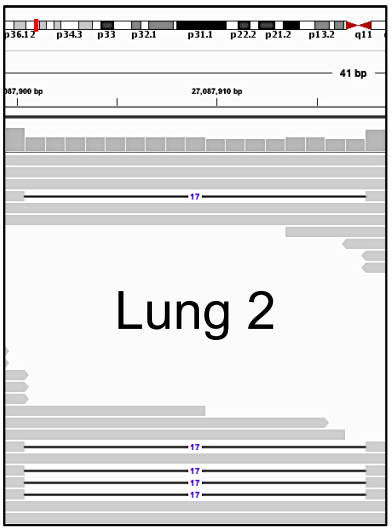

Frameshift mutation 2:
Chr1:27087900

Supplementary Figure 6. Example of ARID1A deletion heterogeneity within patient UTUC1 between primary and metastatic specimens.
Frameshift mutations across tumor samples were examined based on our predicted deleterious analysis. Upon discovery of disparate frameshift mutations in the primary (Chr1:2717094, 2bp) and all metastases (Chr1:27087900, 17bp), the raw BAM files were examined in IGV 2.4.9 (Integrated Genomics Viewer). This revealed the 17bp frameshift mutation was present in the primary sample in one single sequencing read.

Supplementary Figure 7

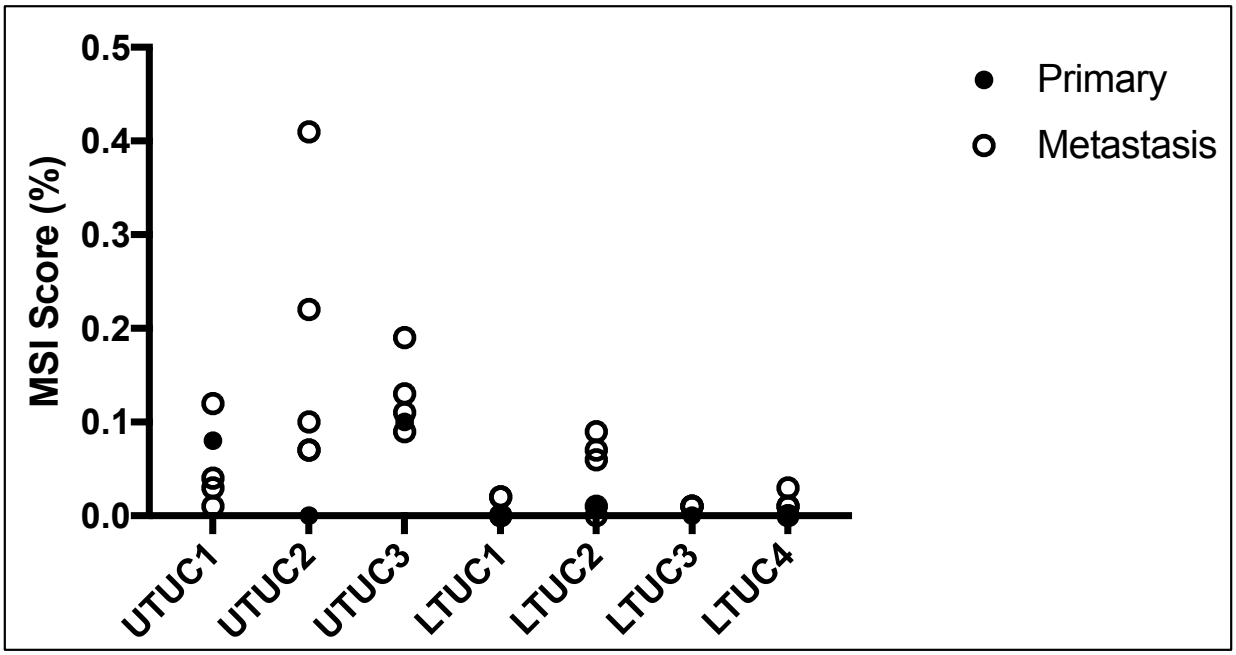

Supplementary Figure 7. MSIsensor microsatellite instability scores for each LTUC and UTUC tumor.

An MSI score of <4% suggests the absence of microsatellite instability.

Supplementary Figure 8

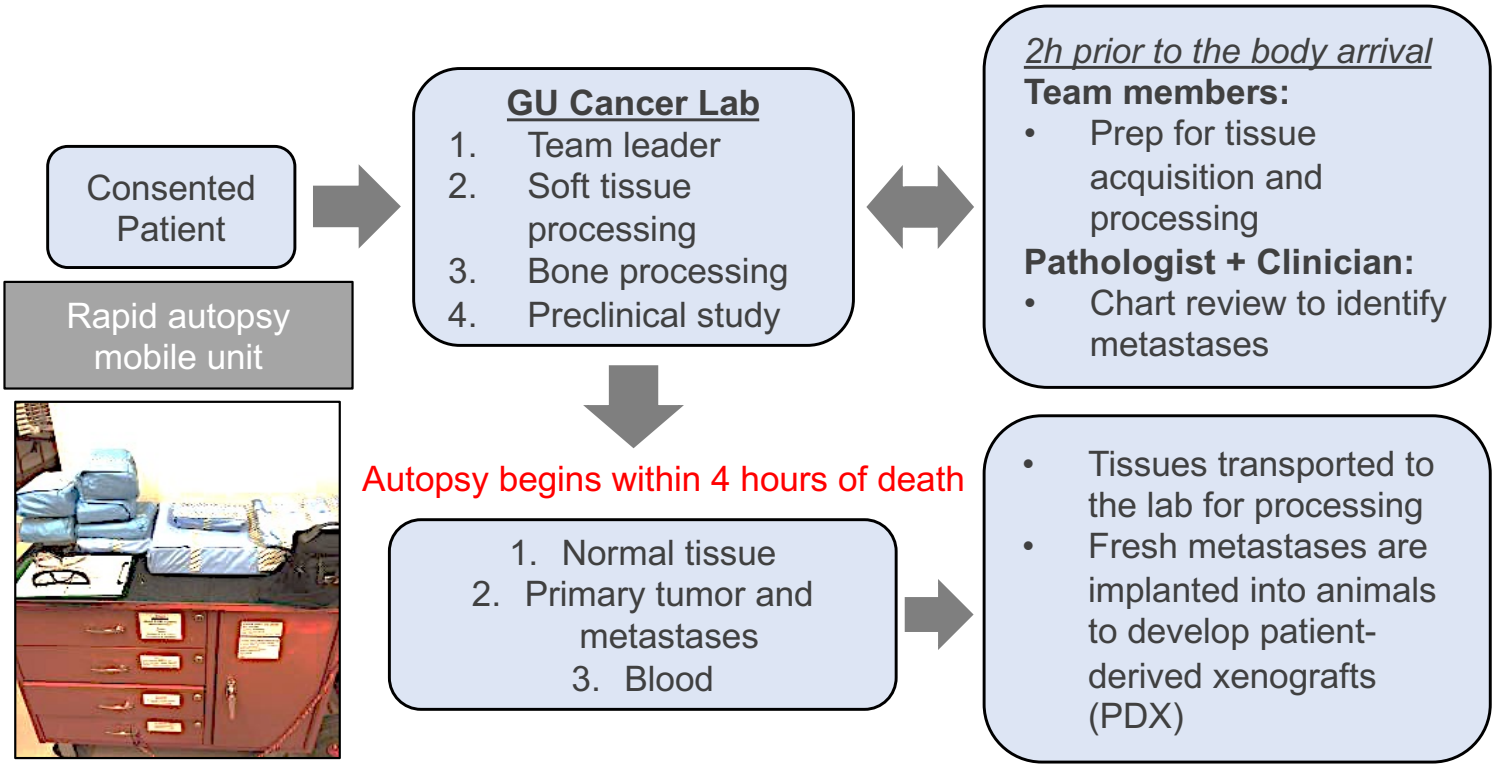

Supplementary Figure 8. Schematic protocol for the University of Washington Bladder Cancer Rapid Autopsy Program.

Supplementary Figure 9

A.

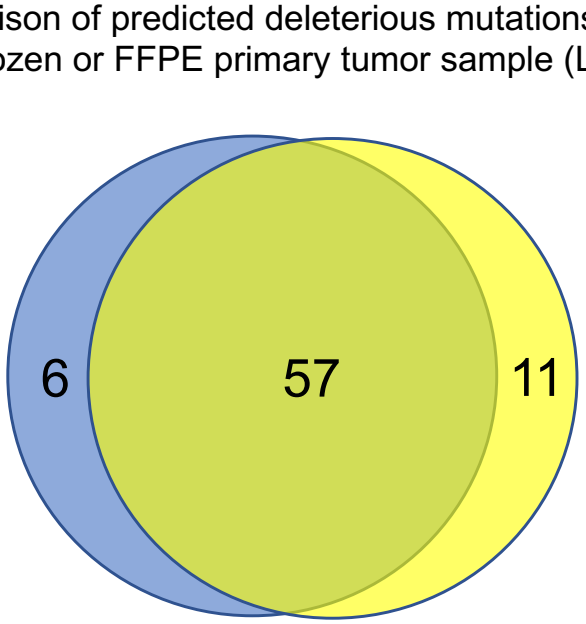

B.

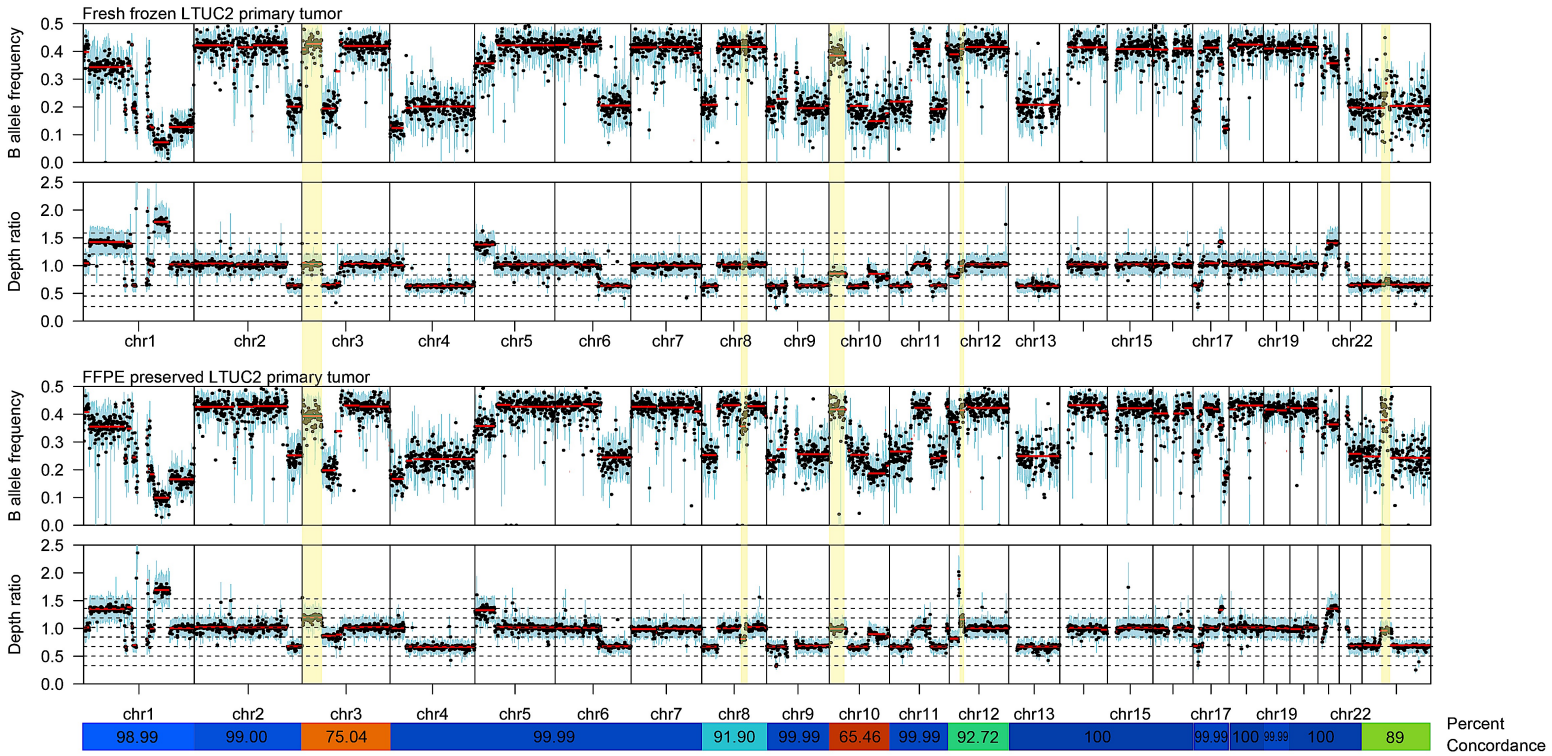

Supplementary Figure 9. sSNV and sCNV profile between FFPE preserved and fresh frozen primary tumors are highly congruent.
As a quality control measure, we evaluated the sSNV and sCNV variations from a single tumor which was bisected. Half was formalin-fixed, paraffin embedded and half of was fresh-frozen. This revealed 80% concordance at the predicted deleterious sSNV level demonstrating only a limited impact of the different preservation techniques on our analysis (A). We also evaluated the genome wide allele specific absolute copy number profile of each sample, with our analysis showing excellent genome wide copy number concordance (B). Both of these findings suggest the differential mode of tissue preservation had limited impact on our analyses.